Exploration Strategies and Feature Prioritisation in Contour-based Haptic Perception of 2D Shape

Lisa P.Y. Lin, Alap Kshirsagar, Boris Belousov, Tim Schneider, Jan Peters, Katja Doerschner, and Knut Drewing

***Abstract*—Perception through touch relies on active exploration strategies that adapt to perceptual goals and object properties. We investigated how information gathering through exploratory procedures (EPs) is organised in haptic shape perception, in particular with respect to the selection of EPs and the prioritisation of shape features - and how these processes are influenced by material properties. In two experiments, participants used a single finger to explore rigid or deformable shapes and judged shape similarity. In Experiment 1, analysis of EPs showed that while contour-following was the dominant strategy for acquiring shape information, participants flexibly supplemented it with additional EPs such as tapping and scanning when exploring deformable shapes. In Experiment 2, trajectory and force data showed a mostly consistent prioritisation of concave regions across exploration parameters (dwell time, velocity, distance, force), regardless of material. Force was modulated by material properties, with participants applying more force to rigid shapes and less to deformable ones. Analysis of the temporal sequence of movements further showed comparable contour-following patterns across materials, but slightly more fragmented movements for deformable shape and smoother, more complete contour tracing for rigid ones, and some shape-specific effects. Together, the findings demonstrate that haptic shape perception is both adaptive and structured: exploratory strategies adjust to material contexts, yet perception and exploration remain anchored by stable geometrical cues, particular concavities, supporting reliable shape perception across contexts.**

***Index Terms*— active exploration, active touch, shape perception, exploratory procedures, haptics, psychophysics.**

L.L, KaD, A.K and J.P were supported by Deutsche Forschungsgemeinschaft (German Research Foundation, DFG) under Germany's Excellence Strategy (EXC 3066/1 "The Adaptive Mind", Project No. 533717223). KaD and KnD were supported by Deutsche Forschungsgemeinschaft (DFG, German Research Foundation) – project number 222641018 – SFB/TRR 135, A5 & B8. *(Corresponding author: Knut Drewing).*

Lisa Lin, Katja Doerschner, Knut Drewing are with Department of Psychology, Justus-Liebig-University Giessen, Germany (e-mail: pui.lin@psychol.uni-giessen.de; katja.doerschner@psychol.uni-giessen.de; knut.drewing@psychol.uni-giessen.de). Alap Kshirsagar is with is with Intelligent Autonomous Systems, Computer Science Department, TU Darmstadt, Germany (e-mail: alap.kshirsagar@tu-darmstadt.de). Boris Belousov is with the German Research Center for Artificial Intelligence (DFKI), Systems AI for Robot Learning (SAIROL), Saarbrücken, Germany, and also with Intelligent Autonomous Systems, Computer Science Department, TU Darmstadt, Germany (e-mail: boris.belousov@robot-learning.de).Tim Schneider is with Intelligent Autonomous Systems, Computer Science Department, TU Darmstadt, Germany, and also with LIRIS, École Centrale de Lyon, Écully, France (e-mail: tim.schneider1@tu-darmstadt.de). Jan Peters is with Intelligent Autonomous Systems, Computer Science Department, TU Darmstadt, Germany, also with the German Research Center for Artificial Intelligence (DFKI), Systems AI for Robot Learning (SAIROL), Saarbrücken, Germany, and also with the Hessian Centre for Artificial Intelligence, Darmstadt, Germany (e-mail: peters@ias.tu-darmstadt.de).

I. INTRODUCTION

Shape perception through touch plays an important role in how we interact with the world. Whether it is reaching into a bag to locate a pen or identifying objects without vision, humans can perceive and discriminate familiar and unfamiliar shapes by touch. This ability relies on active, purposeful hand movements that are finely tuned to both an object's material properties and the specific type of information being sought [1-4]. Through such exploration, humans gather and integrate sensory input to construct shape representations, yet the strategies guiding this process and the features they prioritise when constructing shape representations are less well understood.

These movements are known as exploratory procedures (EPs), which are distinct movement patterns used to extract specific object properties. [3-4]. For instance, contour-following is typically used to extract shape information, lateral motion for texture, and pressure for compliance. EPs are effective and efficient, and people habitually select strategies suited to the property they aim to extract [3, 5-6]. However, real-world objects rarely vary along a single dimension. Even when shape is the target of exploration, other properties such as texture and deformability are often present and may influence how people explore. While the role of perceptual goals in shaping EP selection is well established [3-6], less is known about what is central to EP strategies and what changes when humans are confronted with varying object properties that are not central to the task at hand.

Beyond which strategies are used, an equally important question is how humans organise the shape information they acquire. Shapes are made up of distinct local features such as concavities, convexities, and flat regions, which may differ in their informativeness for perception. Do humans perceive shapes as a unified whole, or do they break them into parts and prioritise certain features when building shape representations? Research on curvature perception has shown that people can reliably detect and discriminate subtle differences in geometry [7-11]. Evidence from vision research suggests that high-curvature areas often contain important structural information that supports shape decomposition and recognition [12-13]. For instance, convex regions have been linked to shape segmentation and recognition [14-17], while concave regions are often associated with defining part boundaries and enabling the decomposition of complex shapes into components [18-20]. Some studies suggest that both features together, or the transition between them may also contribute, depending on the context and stimuli [13, 20-23]. Consistent with this, haptic

studies suggested that perceivers may simplify complex shapes into familiar geometrical components when constructing mental representations [24-25]. Together, these findings raise the possibility that haptic shape perception may similarly rely on feature prioritisation during exploration and on feature-based organisation when forming shape representations.

Furthermore, both strategy selection and feature prioritisation unfold in interaction with the physical properties of the object being explored. Previous studies in vision have shown that material properties can subtly influence shape perception. For instance, velvet-covered or translucent shapes are perceived as flatter or less curved than identical shapes made of matte or opaque materials [26-27]. Suggesting that shape perception may be influenced not only by geometry, but also by material characteristics. In touch, such influences are likely to emerge through changes in exploratory behaviour. For example, the texture or compliance of an object can alter how people move their fingers and the spatial/shape relevant information they can extract. In [36] it has been demonstrated that higher deformability of materials comes along with longer exploration time in shape perception. Other previous studies have shown that EP usage depends not only on material or task in isolation, but also on their interaction [5], showing that haptic exploration flexibly adapts to both task demands and material properties. Material-driven adjustments may in turn shape how information about an object's form is gathered and organised. It remains unclear which aspects of exploration are essential for forming shape representations and whether such adjustments ultimately affect shape perception itself.

Therefore, in the present study, we investigated how people organise and adapt their haptic exploration when perceiving shapes, focusing on EP selection, feature prioritisation, and temporal organisation of movement. Across two experiments, we asked to what extent these strategies are shaped primarily by the perceptual goal of extracting shape information, and whether they are also modulated by material properties. Specifically, the differences between rigid and deformable shapes. In Experiment 1, we examined EP usage during shape perception, whether it varies with materials, and how such variations affect the consistency of shape similarity judgements. In Experiment 2, we examined how shape information is gathered and organised, asking whether people preferentially explore certain local shape features (concave, convex, flat regions), and how their movements unfold over time along the object's contour. We chose stimuli of a handy size that are large enough to require active sequential exploration when using a single finger. Together, these experiments aimed to characterise the organisation of haptic shape perception in terms of strategy selection, feature prioritisation, and temporal structure of exploration, and to test how flexible these processes are in adapting to material contexts. From previous findings, we expect that people prefer curvature regions over flat ones, and that deformable objects would need more effort to explore than rigid ones. Portions of this work have been previously presented in the Proceedings of EuroHaptics 2024 [28] and WorldHaptics 2025[29].

II. EXPERIMENT 1

In this experiment, we examined EP usage during shape perception and whether it changes with material properties. Participants explored textured-rigid or silicone-deformable shapes using a single finger. In each trial, they explored one reference object and two comparison objects, before selecting the comparison object they judged to be more similar in shape to the reference. Finger movements during exploration were recorded and later classified into distinct EP categories.

A. Methods

1) **Participants**

10 participants (5 females, M_{age} = 28, SD_{age} = 4.59, range = 21-34 years) from Giessen University participated in the experiment. All but one were right-handed and reported no history of motor or cutaneous impairments. The right index finger two-point discrimination threshold was <4mm for all participants. Written informed consent was obtained, and participants received 8€/hr compensation. Video data from 2 participants were excluded due to recording errors or incomplete datasets. This study was approved by the local ethics committee at Giessen University (LEK FB06) and conducted in accordance with the Declaration of Helsinki (2013).

Fig. 1. Depiction of the experimental set-up, as well as the silicone-deformable shapes (top left panel) and textured-rigid shape sets (bottom left panel) used in the experiment.

2) **Stimulus**

Two sets of stimuli were used: silicone-deformable shape and textured-rigid shapes (Fig. 1). The silicone-deformable shapes were cast from two-component silicone rubber solution (Alpa Sil EH A & B) in 3D printed moulds, with different amounts of silicone oil added to produce five deformability levels: d1:1.13 mm/N (most deformable), d2:1.02 mm/N, d3:0.79 mm/N, d4:0.68 mm/N, d5:0.44 mm/N (least deformable). The textured-rigid shapes were 3D printed and covered with one of the five fabrics: t1: corduroy, t2: tweed, t3: velvet, t4: jersey cotton, t5: burlap. Texture labels were assigned randomly and do not correspond to any physical ordering.

Each stimulus set contained two subsets (A and B) created by pairing different shapes with specific deformability or texture levels, producing different

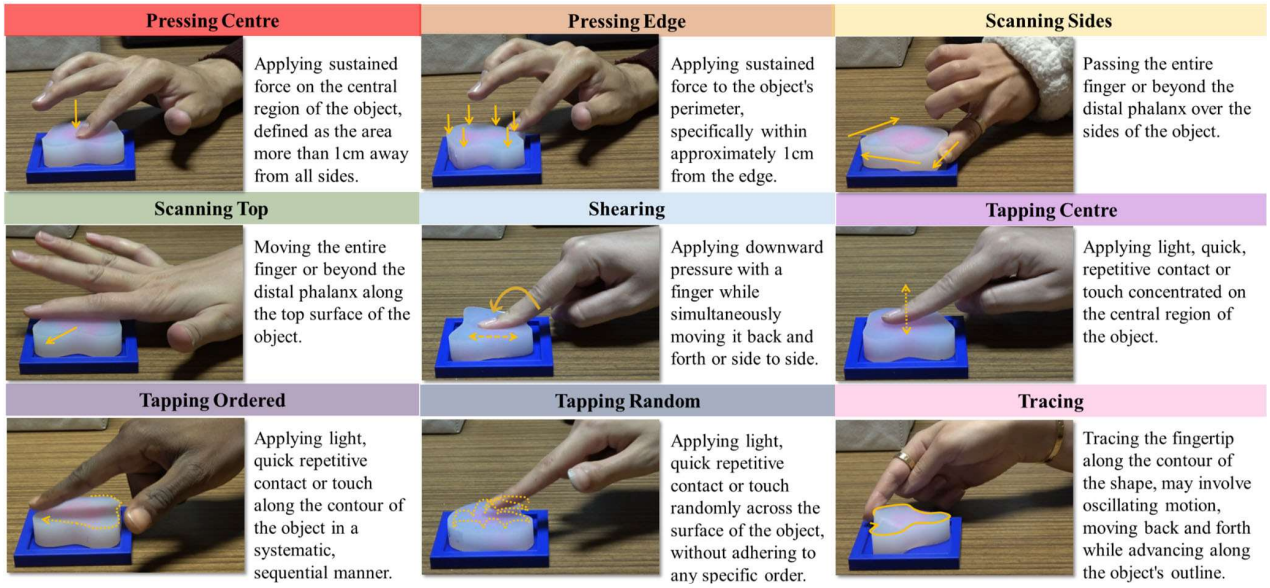

Fig. 2. Description of the EPs proposed in this experiment. Yellow arrows depict the direction and trajectories of movement.

texture × shape and deformability × shape combinations– to prevent the learning of specific level pairings.

Each subset consisted of five shapes (approx. 60 × 60 ×20 mm). We aimed for non-symmetrical shapes because symmetry may induce unwanted top-down processes. First, a batch of irregular shapes were generated. Second, by face validity of three authors (LL, KaD, KnD) we selected 5 shapes that were clearly distinct, not too complex and varied in number and prominence of curvature elements. Shapes were labelled arbitrarily (e.g., shape1, shape2), unrelated to their features.

3) **Apparatus**

Participants sat at a table facing the experimenter. The experience, programmed in PsychPy (v2022.2.4), was controlled from a monitor and keyboard positioned to the experimenter's left. Hand movements were recorded with a Sony Digital 4K video camera (1920 × 1080 px, 28-bit), mounted on a tripod to the left of the table. Each stimulus was placed in a 3D printed tray (65 × 65mm) fixed to the table, with a thin silicone lining to minimise displacement during exploration.

4) **Design and Procedure**

Participants completed two conditions across two consecutive days, each lasting approximately 1.5-2 hours. In one condition, they explored the texture-rigid shapes; in the other, they explored the silicone-deformable shapes. Condition order was counterbalanced across participants.

Each condition began with 10 practice trials, followed by 2 test blocks. Each test block used one stimulus subset (A or B), with block order randomised. Each subset consisted of five shapes, from which 20 distinct reference × comparison object combinations were generated. To ensure comprehensive coverage, each shape served as the reference object four times, with the remaining shapes acting as comparison objects twice. All combinations were presented once per block in randomised order. Participants completed 2 test blocks per condition, resulting in a total of 80 trials.

After providing informed consent, participants were blindfolded and completed the two-point discrimination test on the right index fingertip. The experimenter applied the tips of a two-point discriminator wheel at varying distances (2-8mm) and asked participants whether they felt one or two points. Each distance was presented multiple times in descending order, until participants could no longer consistently report two distinct points across repeated trials. The smallest distance at which two points were still reliably distinguished was recorded as the discrimination threshold.

They then received instructions for the shape similarity tasks. In each trial, participants sequentially explore a reference object and two comparison objects. A trial began with participants placing their right hand on the table, palm facing upwards. On the experimenter's signal, they explored the reference object with their right index finger at their own pace. Participants were not given further instructions on how to explore the objects to avoid biases in their explorations. Exploration ended when they placed their hand back on the table, signalling to the experimenter to present the next object. This process was repeated for the first and second comparison objects. After all three objects had been explored, participants verbally indicated whether the first or second comparison object was more similar in shape to the reference.

Note: In the original study design, participants completed two sessions: one with silicone-deformable shapes and one with textured-rigid shapes. Each session included 4 blocks: 2 shape judgement blocks and 2 blocks involving judgements of other object properties (deformability for deformable shapes, and texture for rigid shapes). The 4 blocks were presented in a randomised order within each session, session order was counterbalanced across participants. The present paper

reports only the shape judgement blocks, which are directly relevant to the current research question. The context is noted as the broader task structure could have influenced exploration behaviour. However, the design was chosen to counteract any confound from block or session order. Exploratory procedure categories (see *Analysis* subsection) were developed from the full video dataset to ensure all movement types were captured.

B. Analysis

1) **Exploratory procedure (EP) coding:**
To examine whether EP usage varied based on material properties, we categorised participants' finger movements into nine predefined EP based on the full video dataset from the original study. These EP categories were defined prior to the present analysis to capture all movement types across different task contexts. Before video coding, 80 video samples were randomly selected from all participants' recordings across both conditions. The authors and two raters reviewed these videos together to identify recurring movement patterns, which were refined into nine EP categories (see Fig. 2).

2) **Coding Procedure and relative EP durations**
For the silicone-deformable dataset, one rater coded all videos, with a second rater independently coded 50% of the videos to assess interrater reliability. For the texture-rigid dataset, one rater coded all videos, and two additional raters each coded 25% of the same videos. Interrater reliability was high (Cronbach's α = .992 -.994), indicating consistent coding across raters. Cronbach's α was used as it provided a measure of consistency across multiple raters, rather than just pairwise correlations. Each EP occurrence was annotated with start and end time points for each trial. The relative duration of an EP was calculated by dividing its total duration by the sum of all EP durations in the same trial, such that all relative durations in a trial summed to 1. These relative EP durations were averaged across raters and used in all subsequent analyses.

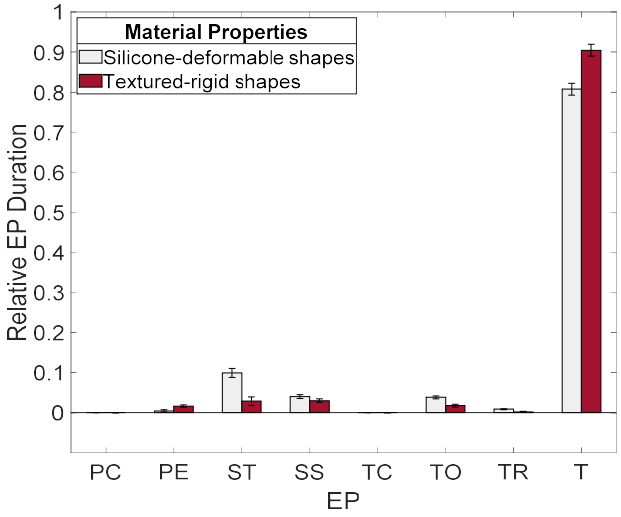

Fig. 3. Relative EP durations plotted as a function of material properties (silicone-deformable vs. textured-rigid). **PC** = pressing centre, **PE** = pressing edge, **ST** = scanning top**, SS** = scanning sides, TC = tapping centre, **TO** = tapping ordered, **TR** = tapping random, **T** = tracing. The EP shearing was omitted from the plot as it was not used. Error bars ± 1SE.

3) **Data Analysis**
   a) *Relative EP durations*: A MANOVA was conducted on the individual relative EP durations to examine whether EP usage varied as a function of the material properties of the shapes (silicone-deformable vs. textured-rigid).
   b) *Similarity judgements*: We computed Cronbach's α between participants for each reference object × comparison objects combination to assess the interparticipant consistency of their perceptual judgements in each condition. We also examined how often an object was judged to be most similar to a given reference object by analysing the instances in which an object was judged as more similar when compared to another. To do this, we counted the number of such occurrences and divided it by the total number of comparisons.

C. Results

1) **EP Patterns across material conditions**
We conducted a MANOVA to investigate the effects of material properties on EP patterns during shape judgements, where the relative durations of the nine EP were the dependent variables and the material property (Silicone-deformable/Textured-rigid) was the independent variable. Analysis revealed a significant effect of material properties on EP patterns, $F(7,632)$, $p < .001$, Wilk's $\Lambda = 0.91$, $\eta_p^2 = .09$, indicating that EP durations differed based on the material properties. Univariate ANOVAs indicated significant differences in EP durations across material properties for all EPs except for 'Scanning sides' and 'Tapping centre', see Table I.

TABLE I
UNIVARIATE ANALYSIS OF VARIANCES ACROSS MATERIAL PROPERTIES

Material Properties	Texture-rigid vs Silicone-deformable shape judgements (Dfs: 1, 638 for all dependent variables)		
Dependent Variable	*F* value	*p* value	η_p^2
Pressing centre	4.802	.029	.007
Pressing edge	9.822	.002	.015
Scanning sides	2.413	.121	.004
Scanning top	20.691	<.001	.031
Shearing	-	-	-
Tapping centre	3.391	.066	.005
Tapping ordered	15.023	<.001	.023
Tapping random	18.435	<.001	.028
Tracing	21.208	<.001	.032

Note: The EP 'Shearing' was not observed during shape judgements, hence there were no results pertaining to this specific EP.

Our results suggest that EP usage during shape perception was influenced by material properties. Although tracing was the most commonly used EP across both material conditions, participants also utilised additional EPs such as 'Scanning Top' and 'Tapping

ordered' more often when exploring silicone-deformable shapes (See Fig. 3). Furthermore, to assess whether the overall patterns of EP used were consistent across materials, we correlated the mean duration of the nine EPs between material conditions. The correlation was very high ($r = 0.996$, $p < .001$), indicating that, despite material-dependent adjustments in specific EPs, the overall pattern of exploration was highly similar across conditions, with tracing dominating both.

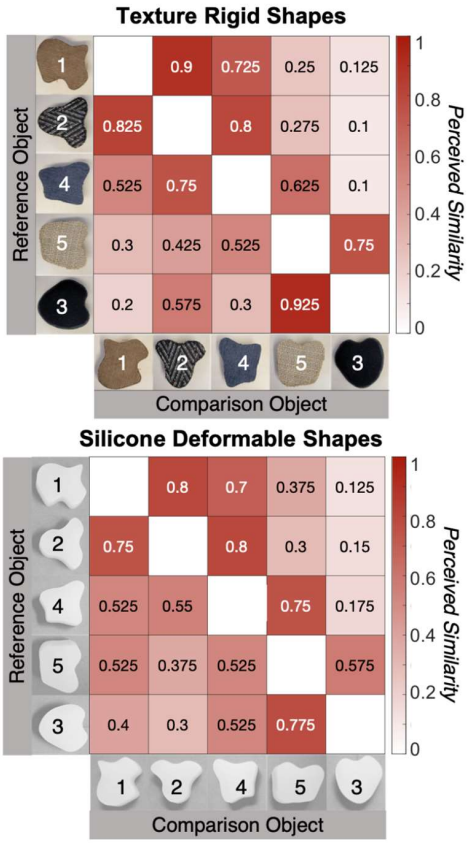

Fig. 4. Perceived similarity in textured-rigid (top) and silicone-deformable (bottom) shape judgments. Similarity matrices illustrate how often an object was rated as most similar to a given standard object; light colours indicate lower values and darker colours higher values.

2) **Similarity Judgements**

We assessed interparticipant consistency in shape similarity judgements across material conditions. Cronbach's α values were 0.476 for silicone-deformable shapes and 0.758 for textured-rigid shapes, indicating lower consistency among participants for deformable shape judgements compared to rigid ones. We also examined the frequency with which object was selected as most similar to a given reference object. In Fig. 4 we visualised these patterns of perceived similarity across material conditions. Despite the lower within-condition agreement for deformable shapes, the similarity matrices for the two material conditions were strongly correlated ($r^2 = 0.85$, $p < .001$), indicating that, on average, participants perceived the relationships between shapes consistently regardless of material variations.

C. Discussion of Experiment 1

In this experiment, we investigated EP usage during shape perception and whether it varied with material properties. EP patterns differed slightly across conditions: when exploring textured-rigid shapes, tracing dominated the EP patterns, whereas when exploring silicone-deformable shapes, participants often supplemented tracing with EPs such as tapping and scanning. Although these additional EPs were not exclusive to deformable shapes, they occurred more frequently in that condition, suggesting that participants adapted their exploration strategies to the object's material properties.

Still, tracing remained the primary strategy in both materials, suggesting that participants employed a consistent approach to extract shape information. The supplementary EPs observed for deformable shapes likely served as a way to stabilise perception when direct contour-following/tracing was less reliable. For instance, participants may have used scanning and tapping to probe the surface more gently to obtain complementary cues about the object's overall shape, thus allowing them to perceive shape without distorting the deformable material. In line with this, the overall pattern of EP usage was highly similar across materials ($r = .996$, $p < .001$), suggesting that while participants adjusted specific movements to accommodate material differences, the underlying structure of their exploration strategy was preserved.

We also assessed participants' shape similarity judgements. Interparticipant consistency was lower for silicone-deformable shapes compared to textured-rigid shapes. This reduced agreement may reflect the added variability introduced by combining different levels of deformability with shape differences, which could make it more difficult to form stable shape representations across participants. Nevertheless, despite this lower within condition agreement, the similarity matrices of the two material conditions strongly correlated when individual noise is reduced by averaging. These findings suggest that while material properties influenced exploration behaviour, reduced agreement and exact individual processing, when deformability levels varied participants may still have relied on stable underlying geometric cues and shape features when forming representations. These could yield consistent averaged judgements despite differences in material contexts.

To examine this possibility, in Experiment 2, we shifted focus to how participants gathered shape information in more detail, testing whether they systematically prioritise specific local shape features (concave, convex, flat regions), how they organised their movements along the shape's contour over time, and whether these exploration patterns generalise across rigid and deformable materials.

III. EXPERIMENT 2

In this experiment, we examined whether participants systematically prioritise certain local shape features during haptic exploration and how their exploration unfolded over

time. Using the same sets of shapes as in Experiment 1 but with simplified material manipulation (rigid 3D printed plastic shapes without textures, and deformable silicone shapes with a single compliance level), we analysed participants' exploration patterns (dwell time, cumulative distance, velocity and force) across concave, convex and flat regions of the shapes. As well as the temporal organisation of their movements, quantified using three sequence-based measures: reversals (back-and-forth movement between neighbouring regions), jumps (movements between non-neighbouring regions), and coverage (the extent to which the entire contour was explored). We also assessed the consistency of participants' shape similarity judgment across these material conditions.

A. Methods

1) **Participants**

18 participants (4 males, aged 18-30, M_{age}= 22.9, SD_{age}= 3.1) were recruited from Giessen University. Three were left-handed, all others were right-handed, and none reported motor or cutaneous impairments. All participants had a two-point discrimination threshold of <4mm on their right index finger. All participants provided informed consent and received 8€/h for participation. One participant was excluded due to equipment issues, leaving a final sample of 17 participants. This study was approved by the ethics committee at Giessen University (LEK FB06) in line with the Declaration of Helsinki (2013), except for preregistration.

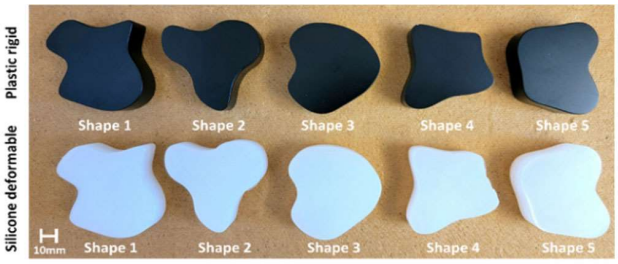

Fig. 5. Stimuli in the current experiment. Top row: Plastic-rigid shapes. Bottom row: Silicone-deformable shape.

2) **Stimulus**

Two sets of stimuli were used: silicone-deformable shapes and plastic-rigid shapes (Fig.5). Silicone-deformable shapes were cast from 3D-printed moulds using a two-component silicone rubber solution (Alpa Sil EH A & B) mixed with silicone oil. The compliance level of the silicone-deformable shapes was 0.68 mm/N [30]. Plastic-rigid shapes were 3D-printed and were polished to minimise any lines or texture left by the printing process. Unlike in Exp. 1 stimuli of each set did not vary in another dimension than shape. The same base shapes as in Experiment 1 were used. Each set contained five shapes (approx. 60×60×20mm) that varied in the number and prominence of curvature elements. Shapes were labelled numerically (e.g., shape 1) with labels assigned arbitrarily and unrelated to their physical or geometrical properties.

3) **Apparatus**

Experiment 2 took place at a visual-haptic workbench equipped with a PHANToM 1.5A haptic device (spatial resolution: 0.03mm; temporal resolution: 1000Hz, friction of 0.04N and inertia of <75g, which is negligible in the present experiment) to track finger position. A force sensor (measuring beam LCB 130, amplifier GSV-2AS, 682Hz; 0.05N, ME-Messsysteme) was placed beneath the stimuli via a custom-made mount to record the force exerted during exploration. The visual scene was presented on a 24-inch computer screen (120Hz, 1600×900pixels), displaying a scene that corresponded to the physical locations of the stimuli (Fig. 6).

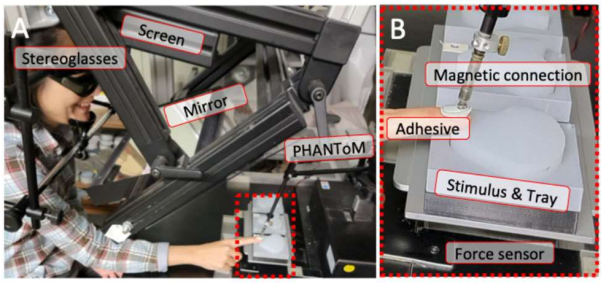

Fig. 6. A) Participant performing the experiment (note: lights on for illustration; lights were off during actual trials). B) Close-up of the magnetic finger attachment to the PHANToM and the custom stimulus platform mounted on the force sensor.

In the visual scene, each stimulus was represented by a grey circular disc, and participants' finger position was represented by a green sphere. These visuals guided finger position before exploration and disappeared upon contact with the stimulus, which had not been possible in the setup of experiment 1. No visual feedback was provided during exploration.

Participants wore stereo-glasses (CrystallEyesTM) and viewed the screen via a mirror, with head position stabilised by a chin rest. Their right index finger was connected to the PHANToM via a magnetic attachment secured to the fingernail (Fig. 6B), allowing six degrees of freedom in finger movement while keeping the fingertip pad free for tactile exploration. The devices were connected to a PC that controlled the experiment and recorded finger positions and applied force at a temporal resolution of 3ms. Noise-cancelling headphones (Sennheiser HD 280 Pro) played white noise to mask background sounds and delivered beeps to signal the start and end of each exploration period.

Each stimulus was placed in a shape-specified tray (80×63.3×15mm) with a 1mm clearance, allowing it to protrude by 10mm above the surface to minimise displacement during exploration. For each trial, three trays were mounted side by side on a 3D-printed platform (80×240×15mm) with a metal base attached to the force sensor: reference object on the left, first comparison in the centre, and second comparison on the right, spaced ≈3cm apart. Stimuli were presented in a fixed orientation, determined by the shape-specific trays used to stabilise placement. This ensured consistent positioning but did not allow for testing the effects of orientation variability.

4) **Design and Procedure**

Participants completed two conditions in one session: plastic-rigid shapes and silicone-deformable shapes, with the order counterbalanced across participants. The design

was the same as in Experiment 1, except that each stimulus set comprised only one set of five shapes (rather than 2 subsets). For each stimulus set, we generated the same 20 reference × comparison object combinations used in Experiment 1, in which each shape served as the reference object four times, with the remaining shapes as comparison object twice.

In each trial, participants used their right index finger to explore a reference object and two comparison objects sequentially, then selected the comparison object they perceived as most similar to the reference object's shape. In contrast to experiment 1, the three objects were not presented at the same location but next to each other, and each object was explored for a defined time of 15s, instructed by signal tones. This was an amply time limit allowing for relatively unconstraint, natural exploration behavior. The 20 reference ×comparison objects combinations were presented once per condition in randomised order. Participants completed 20 trials per condition, resulting in a total of 40 trials, lasting about 1-1.5hrs. The experimental session began with participants providing informed consent and demographic information, followed by measuring the two-point discrimination threshold on the right-index finger using a two-point discriminator.

In the visual scene, stimuli were represented by a grey circular disc that turned red to cue finger placement. At the start of each trial, the left disc (reference object) turned red and disappeared immediately upon contact, before any haptic exploration began. The disc served only as a generic positional cue and was not visually informative about the stimulus shape. Participants then explored the object until an auditory beep signalled the end of the exploration period. The same procedure was followed for the centre (first comparison) and right (second comparison) objects. After exploring all three objects, a decision screen appeared and participants selected the comparison object they perceived as most similar to the reference object's shape by pressing a virtual button.

B. Analysis

To characterise the organisation of haptic exploration, analyses were conducted at two levels. Firstly, we examined feature-based measures (e.g. dwell time) to assess how exploration varied across local shape features. Secondly, we analysed the temporal organisation of exploration sequences, specifically, how participants moved between shape regions over time, using sequence-based metrics (e.g., reversals). Together, these analyses provide a complementary view of both the spatial and temporal organisation of haptic exploration during shape perception.

1) **Curvature Analysis:**
To examine whether touch patterns varied by shape features, we categorised object boundaries into concave, convex and flat regions using a curvature visualisation tool ('CurvatureVisualize' [28-29]). Positive values indicated convexity, negative values indicated concavity, and near-zero values represented flat regions (Fig. 8A). Curvature thresholds were defined from the full range of curvature values observed across all shapes (≈ -88.8 to 191m^{-1}), with flat regions defined as (≈ ±15.9m^{-1}). Remaining values were assigned to convex (> ≈16.2m^{-1}) or concave regions (< ≈-16.2m^{-1}). We choose thresholds for convex and concave categories symmetrically and so that they warrant that participants detect the concavities and convexities with a single finger: In [9] detection

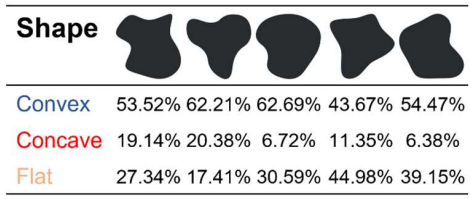

Fig. 7. Shapes are segmented into feature categories based on defined curvature thresholds. Percentages indicate the proportion of each shape's contour per feature type.

thresholds for a single stationary finger were around +/- 5 m^{-1}, and with +/16 m^{-1} convex and concave surfaces were almost certainly distinguished from plane ones (~95%). The thresholds allowed us to segment shape features in a way that preserves perceivable geometric distinctions. To quantify the curvature composition of each shape, we calculated the proportion of the outline corresponding to convex, concave and flat regions. These values are summarised in Fig. 7.

This categorisation was necessary to enable analysis of exploratory behaviour relative to shape features. Segmented features were mapped to PHANToM-derived spatial coordinates, with shape outlines recorded at each experimental location (left, centre, right) and aligned with the curvature-based segmentation to identify feature boundary coordinates for each shape (Fig. 8B).

2) **Data Filtering**
The PHANToM recorded timestamp, finger position coordinates and the applied normal force (N) measured at each timestamp. Each trial involved three stimuli, each placed in its own tray on a platform on top of a force sensor. To isolate participant-applied force, baseline forces (reflecting object weight) were measured and subtracted from recorded data. Force values at baseline indicated no finger contact, while values above the placement or sideways force destabilising the object were treated as artefacts and excluded to ensure only genuine instances of active exploration were analysed.

3) **Mapping Trajectory data to shape feature categories**
Trajectory data points were aligned with the shape's spatial coordinates to determine which parts of the shape each trajectory point corresponded to. While the raw data included timestamped finger position and force measurements, it did not directly indicate which part of the shape was in contact. Misalignments occurred due to natural variations in finger use, with participants sometimes made contact using areas beyond the tracked fingertip (e.g. near the second joint), resulting in small spatial offsets between the recorded trajectories and the actual shape outline (Fig. 8C).

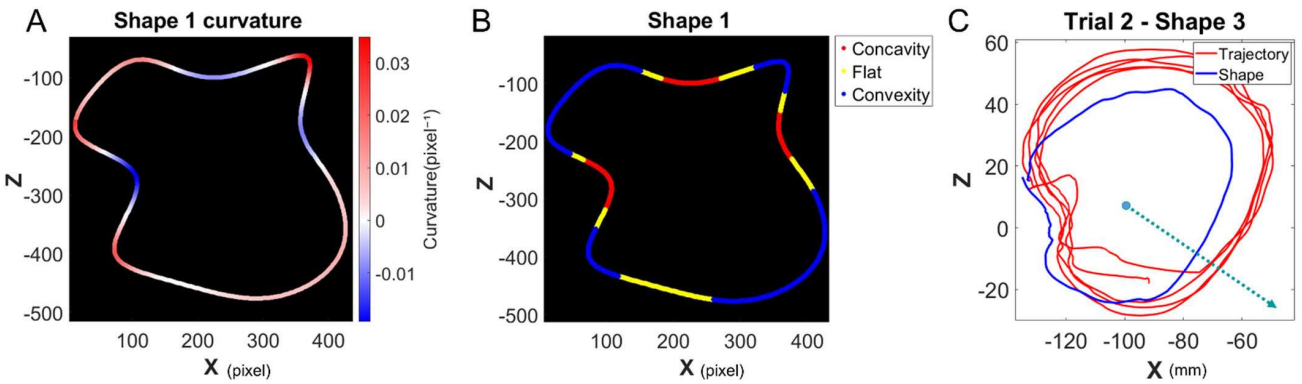

Fig. 8. Curvature analysis and data alignment. A) Shape analysed based on curvature values: positive(red), negative(blue) and near-zero curvature (white), with darker shades indicating greater magnitude. B) Shape segmented into convex (blue), concave (red), and flat (yellow) regions based on the defined curvature thresholds. C) Data alignment schematic: red lines represent trajectory data, blue line shows the shape outline in PHANToM's spatial coordinates (units in mm). Each trajectory point was mapped to the closest point on the outline via a centroid-projected line.

Despite these offsets, the recorded trajectories still closely followed the overall shape contours. To approximate the corresponding location on the shape outline, we used a centroid-based projection method (Fig. 8C dotted line): for each trajectory point, a line was projected from the shape's centroid through the point to identify the closest point on the shape outline along the same radial direction. This process mapped each trajectory point ($X_{trajectory}$, $Z_{trajectory}$) to a corresponding point (X_{shape}, Z_{shape}) on the shape's outline. This method yields an approximate mapping of curvature category, where mapping errors scale with the offset between trajectory and corresponding point. Simulation-derived mapping errors were on average 29% and non-systematic. Using the curvature-based segmentation described earlier, the mapped points were assigned to their respective shape feature category (convex, concave, or flat), enabling analysis of exploration relative to specific shape features..

4) **Data analysis: Feature-based measures**

We extracted exploration parameters: dwell time, cumulative distance, force and velocity for each trial, shape and location. Parameters were computed by shape feature category (concave, convex, flat) based on the segmentation described above.

Relative dwell time: We first calculated dwell time as total time spent on each feature in ms, calculated by multiplying the number of trajectory samples at each XZ coordinate by the 3ms sampling interval then summing across each feature region. From that we computed relative dwell time to account for differences in shape feature proportions, so that our data reflected exploration relative to the size of each feature: We normalised dwell time by dividing the values for each feature by its percentage within the shape. The normalized values show feature prioritization by reflecting the extent of time spent per feature independent of its percentage, and thus discount expectations if participants explored the entire shape in a constant, uniform way.

Relative Cumulative Distance: Cumulative distance in mm is the total distance travelled across each feature. Computed by summing the Euclidean distances between each consecutive trajectory point.

$$Distance = \sqrt{(x_2 - x_1)^2 + (z_2 - z_1)^2} \quad (1)$$

From cumulative distance, we computed relative cumulative distance analogously to dwell time.

Velocity (mm/ms): Speed of touch across shape features, computed by dividing the Euclidean distance between each pair of consecutive trajectory points by the time interval to obtain the instantaneous velocity. These values were then aggregated by shape feature category then averaged to calculate the mean velocity per feature type.

Force (N): Mean normal force during contact, calculated by averaging force readings from trajectory points mapped to that specific feature.

Similarity judgements: same as in Experiment 1.

5) **Data Analysis: Sequence-based measures**

In addition to feature-based exploration parameters, we also quantified the sequence of exploration across shape regions. Building on the curvature-based segmentation and data mapping described above, each shape was divided into numbered regions, starting at the 12 o'clock position and increasing clockwise (Fig. 9). This numbering provided a consistent spatial reference for analysing the order in which regions were visited, independent of their shape feature category. From these exploration sequences, three temporal measures were derived to capture the organisation of touch over time (consecutive letters in examples refer to neighbored regions within the shape):

Reversals: The number of times participants returned to the immediately previous region (A→B→A), which reflects local back-and-forth movements.

Jumps: Transitions between non-neighbouring regions, which indicate discontinuous movements (A→ C, "jumping" over B).

Coverage: The completeness of exploration, calculated as the total number of regions visited during a trial divided by the total number of regions that made up the shape (e.g., if a shape has 10 regions and 25 were visited in the sequence, coverage = 2.5, meaning the shape contour was

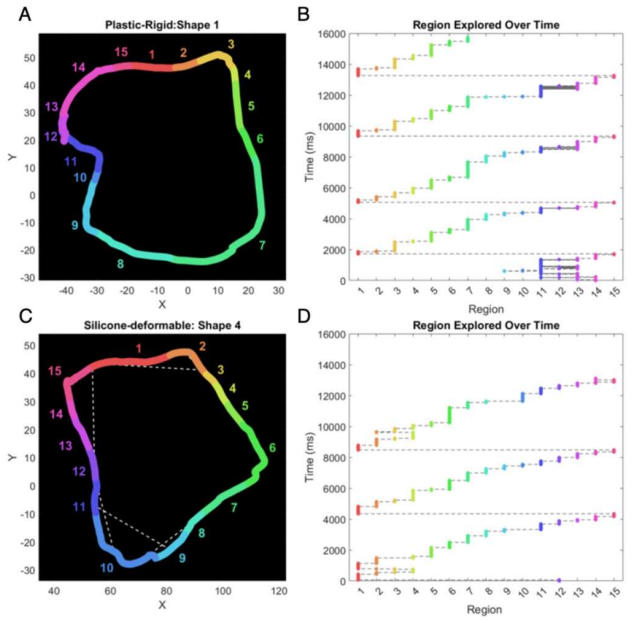

Fig. 9. Example exploration sequences from a single participant in the plastic-rigid (A-B) and silicone-deformable (C-D) conditions. Panel A and C show the spatial segmentations colour-coded by clockwise region order (starting at 12 o'clock). Panel B and D show the corresponding temporal exploration profiles. Exploration was more continuous with greater coverage in the plastic-rigid condition, but more discontinuous with frequent jumps between non-neighbouring regions (white dash lines in panel C) in the silicone-deformable condition.

traced approximately 2.5 times). We analyzed the numbers of reversals, jumps, coverage as function of shape and material in a 2-way repated measures analyses. In addition, we computed normalized values for reversal and jump values in order to study from which features jumps mainly started, and to which features they reverted. Normalization followed the procedure outlined for dwell time in B.4.

C. Results

For the feature-based parameters, a 3-way repeated-measure ANOVAs was conducted with material, shape feature, and shape as independent variables. Touch patterns were primarily influenced by shape features, with concave regions explored longer and more extensively than convex and flat regions across most shapes. Exploration parameters, except for force, remained consistent across material conditions (see Fig. 10).

For the sequence-based measures, a 2-way repeated-measure ANOVA with material and shape as independent variables, showed that the number of reversals was similar across materials, but participants made more jumps between non-neighbouring regions when exploring silicone-deformable shapes. Conversely, coverage was higher for plastic-rigid shapes, indicating more continuous and complete contour tracing (Fig. 13). Normalized values were submitted to another repeated measures ANOVA with feature and material as independent variables.

For all analyses, Greenhouse-Geisser corrections were applied when necessary, Bonferroni adjustment was used for post-hoc tests. To aid interpretation, the Results are organised into three parts: First, the main effects and interactions of material and shape feature on the feature-based exploration parameters. Second, the shape-specific effects and shape×shape feature interactions. Finally, the sequence-based analysis.

1) **Feature-based Exploration Parameters:**

Relative Dwell Time: There was a significant main effect of shape feature, $F(1.11, 17.68) = 131.96$, $p < 0.001$, $\eta_p^2 = 0.89$. Participants spent the most time exploring concave regions compared to convex ($p<0.001$) and flat ($p<0.001$) regions, no significant difference was found between convex and flat regions ($p = .07$, Fig. 10A). A weak main effect of material was also observed, $F(1, 16) = 4.64$, $p = .047$, $\eta_p^2 = .23$, with participants spending slightly more time exploring during the plastic rigid condition ($M = 17198.24$, $SE = 308.82$) than the silicone deformable condition ($M = 16621.02$, $SE = 346.84$, $p = .047$). There was no material × shape feature interaction ($p = .65$).

Relative Cumulative Distance: There was a significant main effect of shape feature, $F(1.13, 18.10) = 92.99$, $p < .001$, $\eta_p^2 = .85$, with concave regions being explored more extensively than convex ($p<.001$) and flat ($p<.001$) ones, no significant difference was found between convex and flat regions ($p = .06$, Fig.10B). A significant interaction of material × shape feature was observed, $F(1.27, 20.34) = 4.53$, $p = .038$, $\eta_p^2 = .22$. For rigid plastic shapes, concave regions were explored more than convex ($p < .001$) and flat

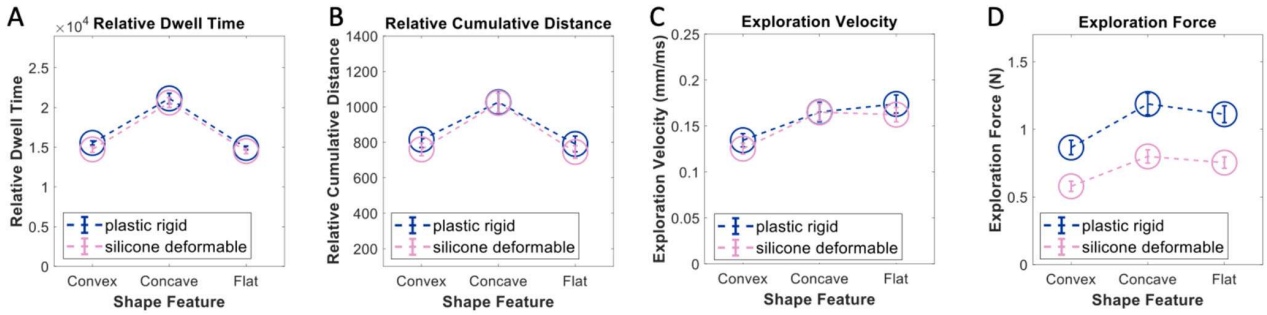

Fig. 10. Exploration parameters plotted as a function of material and shape feature. A) Mean relative dwell time, B) Mean relative cumulative distance, C) Mean exploration velocity, and D) Mean exploration force. Blue lines represent plastic rigid shapes and pink lines represent silicone deformable shapes error bars represent 1± SE.

regions (p< .001), with convex regions explored more than flat regions (p= .002). For deformable shapes, concave regions were explored more than convex (p< .001) and flat ones (p< .001), with no significant difference between convex and flat (p= .62). There was no main effects of material (p = .29).

Velocity: There was a significant main effect of shape feature $F(1.41, 22.53) = 77.57$, p< .001, η_p^2 = .83. Exploration was slowest at convex regions compared to concave (p<.001) and flat (p<.001) regions, with no significant difference between concave and flat regions (p= .9, Fig. 10C). An interaction between material × shape feature was also observed, $F(2, 32) = 6.73$, p= .004, η_p^2= .30, in which for rigid shapes, velocity was slowest at convex regions compared to concave (p< .001) and flat regions (p< .001), with no significant difference between concave and flat regions (p= .07). For deformable shapes, velocity was also slowest at convex regions compared to concave (p< .001) and flat regions (p< .001), there was no difference between concave and flat regions (p= 1.00). There was no main effect of material (p = .23).

Force: There was a significant main effect of shape feature $F(1.21, 19.37) = 51.79$, p< .001, η_p^2= .76. In which convex regions received less force than concave (p<.001) and flat (p<.001) regions, with no significant difference between concave and flat regions (p= .25, see Fig. 10D). There was also a significant main effect of material, $F(1, 16) = 36.34$, p< .001, η_p^2= .70, with participants applying more force to plastic-rigid shapes (M= 1.06, SE= .06) than silicone-deformable shapes (M=.71, SE=.04, p<.001). However, there was no material x shape feature interaction (p = .13). Additionally, a significant interaction of material × shape was found, $F(2.03, 32.54) = 3.65$, p= .04, η_p^2= .19. Although applied force varied slightly across shapes within each material, this did not alter the overall patterns of results: participants applied more force to plastic-rigid shapes compared to silicone-deformable shapes.

2) **Shape-specific effects on exploration patterns**

In this section we report the shape-specific main effects and the shape × shape feature interactions from the repeated-measures 3-way ANOVA. These results suggested distinct exploration patterns for specific shapes (See Fig. 11).

Significant main effects of shape were observed for all parameters, with Shape 5 consistently showed the highest overall values, and significantly exceeding shape 1-4 (ps<.001 for all comparisons): Relative dwell time, $F(1.57,25.09) = 61.38$, p<.001, η_p^2=.79; Relative cumulative distance, $F(1.38, 22.08) = 54.90$, p< .001, η_p^2=.77; Velocity, $F(1.47, 23.49) = 144.50$, p< .001, η_p^2= .90; Force, $F(2.07, 33.04) = 75.01$, p< .001, η_p^2= .82).

Shape × Shape Feature interactions were also significant for all parameters: Relative dwell time, $F(1.92, 30.73) = 64.01$, p< .001, η_p^2= .80; Relative cumulative Distance, $F(1.46, 23.34) = 73.49$, p< .001, η_p^2= .82; Velocity: , $F(1.56, 24.90) = 94.89$, p< .001, η_p^2= .86; and force, $F(2.30, 36.83) = 59.53$, p< .001, η_p^2= .79), showing that exploration across the shape features varied systematically by shape.

Post-hoc comparisons showed a consistent pattern across parameters, in which concave regions were generally explored for longer durations, over greater distances, with higher velocities, and with greater applied force than flat or convex regions (ps<.001-.002). This pattern was observed for all shapes except for shape 3, where flat regions were explored most extensively. For force, shape 4 followed the same general concavity dominant trend, but the difference between convex and flat regions was not significant (p = .40; all other p<.001).

Overall, Shape 5 consistently elicited the highest values across all parameters, suggesting that it may require or encourage more extensive exploration than the other shapes. Conversely, Shape 3 exhibited a distinct pattern in which flat regions dominated exploration, deviating from the general concavity preference. Although both shape 5 and 3 had a similarly small proportion of concave regions (<7%), they differed in how these regions were explored, suggesting that shape feature composition alone may not fully explain shape-specific exploration behaviours. To further understand, we conducted the following analyses:

3) **Effects of Concavity Location on Exploration:**

We hypothesised that the concavity location might explain these differences. Both Shapes 3 and 5 had a single prominent concave region, but Shape 5's concave region was on the right, while Shape 3's was on the left. Since participants used their right index finger for exploration, the left-side concave region may be less intuitive or harder

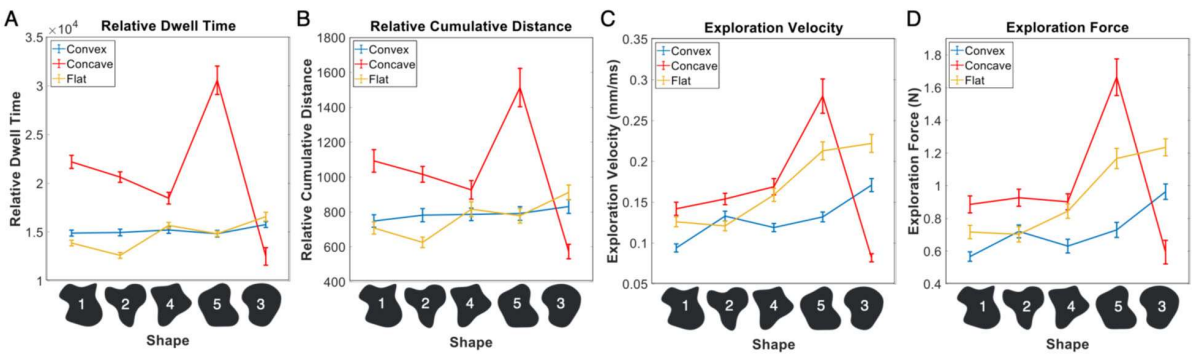

Fig. 11. Shape-specific effects on exploration parameters. A) Relative dwell time, B) Relative cumulative distance, C) Velocity, and D) force, plotted for convex, concave, and flat regions across shapes. Error bars represent 1± SE.

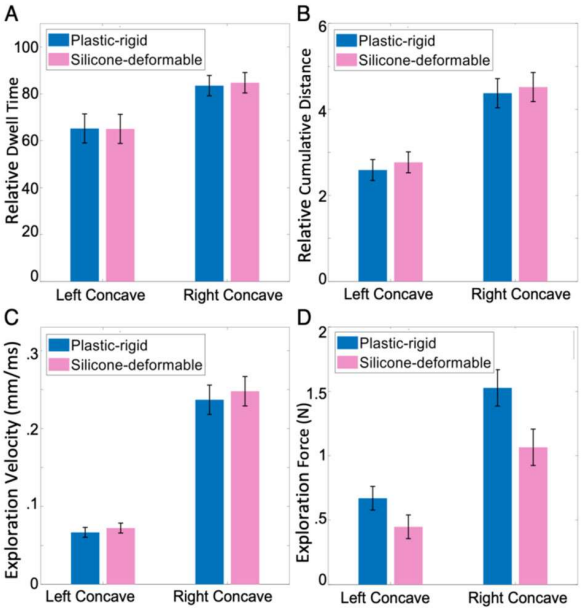

Fig. 12. Exploration parameters plotted as a function of concavity location and material properties. A) Mean relative dwell time, B) Mean relative cumulative distance, C) Mean exploration velocity, and D) Mean exploration force. Error bars represent 1± SE.

to navigate. To test this, we analysed 'Shape 1', which featured two concave regions (one on the left and one on the right). Data were split based on concavity location and averaged across participants, and paired-sample T-tests were performed on exploration parameters. Results showed that the concave region on the right exhibited similar exploration patterns to Shape 5 (See Fig. 12).

Relative Dwell Time: Participants spent significantly more time exploring the right-concavity (M= 84.16, SE= 3.04) compared to the left-side (M= 65.15, SE= 4.32), $t(33) = 3.62$, $p< .001$.

Relative Cumulative Distance: The right-concavity (M= 4.45, SE = .27) was explored more extensively than the left-side (M= 2.68, SE= .17), $t(33) = 7.932$, $p< .001$.

Velocity: Velocity was higher for the right-concavity (M= .24, SE = .01) compared to the left (M= .07, SE= .004), $t(33) = 14.57$, $p< .001$.

Force: Participants applied more force to the right concave region (M= 1.30, SE= .11) than to the left (M= .56, SE= .07), $t(33) = 6.23$, $p< .001$.

Handedness: All right-left effects from a-d were numerically very similar in the 3 left-handed (LH) and the 14 right-handed (RH) participants (Dwell Time, RH: 83 vs. 65, LH: 92 vs. 65; Distance, RH: 4.4 vs. 2.6, LH: 4.7 vs. 3.0; Velocity, RH: .23 vs. .07, LH: .25 vs. .08; Force, RH: 1.29 vs. 0.55, LH: 1.32 vs. 0.62), rejecting the idea that handedness plays a role here.

These results suggested that location of the concave region influenced touch patterns, likely due to biomechanical constraints of exploring with the right index finger.

4) **Sequence-based Measures:**

To further examine how participants organised their exploration over time, we analysed the temporal structure of their exploration using three measures: reversals, jumps, and coverage. These measures characterised how participants progressed through different regions of each shape, e.g. whether they explored locally and repeatedly, moved discontinuously between distant regions, or traced the contour more completely.

Reversals: A main effect of shape, $F(1.24,19.32) = 142.18$, $p <.001$, $\eta_p^2 = .90$, indicated more reversals on Shape 1 than on other shapes (all $ps<.001$). No other effect was significant (ps = .32-.53).

Normalized reversals: There was a main effect of feature, $F(2,34) = 109.65$, $p <.001$, $\eta_p^2 = .87$, with most reversals towards convex parts (M = 3.56, SE = 0.29), least to concave parts (M = 1.09, SE = 0.08) and flat in-between (M = 1.60, SE = 0.17, all $ps<.005$). No other effect was significant (ps = .18-.36).

Jumps: Significant main effects of material, $F(1,16) = 11.97$, $p = .003$, $\eta_p^2 = .43$, and shape, $F(1.03,16.53) = 154.11$ $p <001$, $\eta_p^2 = .91$, indicated that participants made more jumps when exploring silicone-deformable shapes (M = 2.67, SE = .22) than plastic-rigid shapes (M = 1.92, SE = .18). Jumps were also more frequent for Shape 1 ($ps<.001$). The interaction was not significant (p = .65).

Normalized jumps: Significant main effects of feature, $F(2,34) = 165.90$, $p < .001$, $\eta_p^2 = .91$, material, $F(1,17) = 12.30$ p = 003, $\eta_p^2 = .42$, and the interaction feature x material, $F(1.39, 23.6) = 6.019$, p = 014, $\eta_p^2 = .26$, were observed. There were more jumps from convex than from

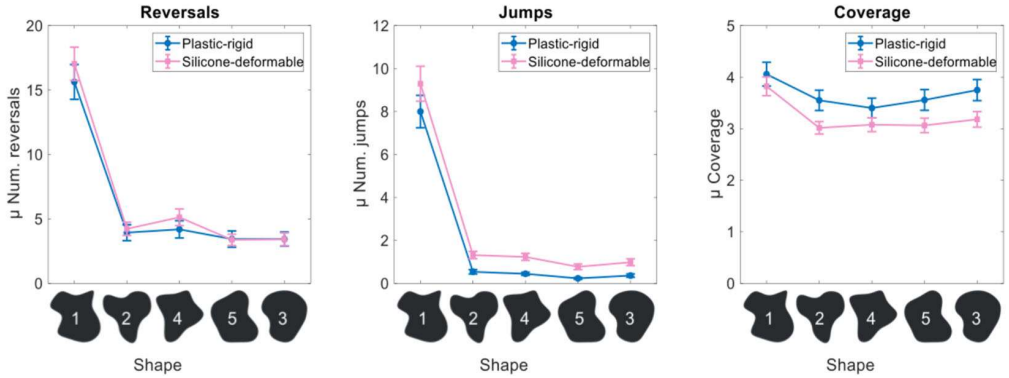

Fig. 13. Sequence-based measures plotted as a function of shapes and material properties. A) Mean number of reversals, B) Mean number of jumps, C) Mean coverage. Error bars represent 1± SE.

concave than from flat parts, more jumps for silicone than plastic stimuli, and this material effect decreased with the number of jumps per feature (silicone vs plastic convex, M = 1.81, SE = .15 vs M = 1.29, SE = .12, concave M = 1.14, SE = .08 vs M = 0.90, SE = .08, flat M = 0.17, SE = .03 vs M = 0.05, SE = .01; all ps<.001).

Coverage: There were main effects of material, $F(1,16)$ = 10.26, p = .006, η_p^2= .39, and shape, $F(1.78, 28.54)$ = 42.10, p <.001, η_p^2= .73. Coverage was greater for plastic-rigid shapes (M = 3.70, SE = .21) than for silicone-deformable ones (M = 3.24, SE = .14) and was highest for shape 1 (ps<.001). The material x shape interaction was not significant (p = .09).

As illustrated in Fig. 13, participants tended to explore plastic-rigid shapes more continuously, often tracing around the contour multiple times, resulting in higher coverage value. Conversely, exploration of silicone-deformable shapes were more fragmented, with more frequent jumps between non-neighbouring regions.

5) **Similarity judgements:**
We assessed how consistent participants were with their shape similarity judgements across material conditions. The Cronbach's α values were .96 for shape judgments of plastic-rigid objects and .97 for silicone-deformable objects, indicating high level of consistency. Fig. 14 visualised the similarity matrices across material conditions. The correlation between similarity matrices of silicone-deformable and plastic-rigid shapes were also strong (r^2 = .87, p< .001), suggesting that participants were not only consistent with their exploration behaviours, but they also perceived the shapes consistently across material conditions.

6) **Similarity judgements across Experiment 1 and 2:**
To assess the generality of shape perception across experiments, we correlated similarity matrices between conditions from Experiment 1 and 2. Correlations were generally high (all r^2 > .85, p< .001), both when comparing corresponding material conditions across experiments (Rigid: r^2 = .93; Deformable: r^2 = .90), and when comparing across materials (rigid vs deformable across experiments: r^2 = .86 -87).

D. Discussion of Experiment 2

In this experiment, we investigated whether participants systematically prioritise local shape features during exploration, how they organised their movement along the shape's contour over time, and whether such prioritisation generalised across material conditions. Across exploration parameters and for most shapes, participants focused more on concave regions compared to convex or flat ones, suggesting that concavities may provide particularly informative cues for haptic exploration. This preference was observed in both rigid and deformable shapes, suggesting that feature prioritisation is robust to material differences.

Exploration behaviour varied slightly with materials; participants applied more force to rigid shapes, compared to deformable ones, which likely reflect an adaptive strategy to enhance tactile resolution on rigid objects while avoiding distortion in deformable ones. In contrast to [36] and our

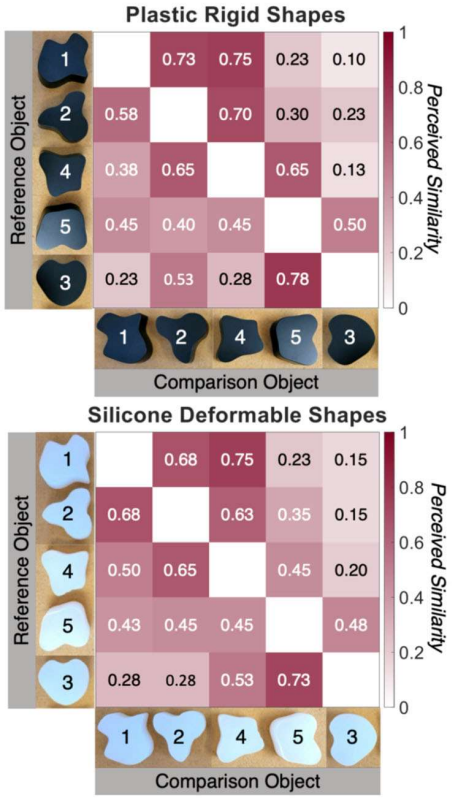

Fig. 14. Perceived similarity in plastic rigid (top) or silicone deformable (right) shape judgments. These similarity matrices illustrate how often an object was rated as most similar to a given standard object; light colours indicate lower values and darker colours higher values.

expectations, we did not find that participants explore deformable objects longer or with more effort, maybe because here they accounted for material differences by force adaptation. Sequence analysis demonstrated that the overall structure of exploration was similar across materials. The number of reversals was comparable, suggesting a consistent contour-following strategy. However, participants made more jumps between non-neighbouring regions when exploring deformable shapes and achieved greater contour coverage for rigid shapes. These patterns suggested modest change due to material constraints/differences, with more fragmented movements for deformable shapes and smoother, more continuous contour tracing for rigid ones. The increase of jumps for silicone-deformable materials could both relate to their compliance or their higher friction, which both interfere with smooth gliding. Despite material-specific effects, the underlying exploration strategy is stably maintained. In the experiment we studied a single deformable material, which had a medium deformability. It is an interesting question whether with more deformable materials we would still see the same overall exploration strategy, but with less force and more fragmentation. Future experiments should also measure shear force in order to better understand potential material-specific

influences on contour following accuracy.

There were shape-specific effects: Shape 5 showed particularly pronounced effects for concave regions, whereas Shape 3 showed a pattern where flat regions were more prominent than concave ones. The follow-up analysis on shape 1 suggests that these shape-specific touch patterns may be due to the to the location of the concavities in Shape 3 (right side), and Shape 5 (left side), likely related to biomechanical constraints of exploring with the right index finger. Further, across material conditions, Shape 1 consistently showed a markedly higher numbers of reversals and jumps than other shapes, despite following the same overall patterns of effect. Examination of where these movements occurred showed that most reversals and jumps were concentrated in region 11-13, an area featuring an abrupt transition from concave to flat to convex. This rapid change in curvature likely disrupted smooth contour following, prompting participants to move back and forth locally or skip across neighbouring regions. Overall, most jumps started at convex regions, but almost none at flat regions, Most reversals also went back to convex regions. At the same time concave regions were explored most intensively in terms of time, distance, force. We hence speculate that jumps and reversal may mainly have biomechanical causes, in that people might unintendedly loose contact with convex parts, also by jumps and then revert to further explore. In contrast it might be easier to keep the finger within a concave region. However, the fact that participants revert to convexities also suggests that these have some perceptual relevance.

Shape similarity judgements showed high interparticipant agreement within each condition, and strong correlation across rigid and deformable shapes. Additionally, similarity matrices were highly correlated not only within experiment, but also when compared across experiments. This suggests that participants' shape judgements were guided by stable geometrical cues that generalised across different participant samples, stimulus manipulations and experimental contexts. Remember that in experiment 1 the stimuli in each trial did not only differ in shape, but also in judgement-irrelevant properties (texture, deformability). The finding of similar overall shape judgments across experiments hence particularly corroborates the idea of stable cues. At the same time the variability of judgement-irrelevant properties in experiment 1, explains why interindividual judgment consistency was lower than in experiment 2: Judgment-irrelevant properties likely influenced shape judgments, but differently for different participants because of individual exploratory behavior or perceptual weightings. In a similar way we had explained why consistency in experiment 1 was lower for deformability as compared to texture variation: namely, because exploration differences cause larger shape uncertainty for differently deformable objects as compared to rigid ones with different textures. Still it is important that average judgments were highly correlated, so that we can assume stable underlying geometric cues despite individual differences in exact processing.

Taken together, these findings demonstrated that participants mainly prioritise concavities during exploration, adjusted their touch patterns to material properties, and perceived shapes consistently across different material contexts.

IV. GENERAL DISCUSSION

We investigated how people organise haptic exploration when perceiving shapes, examining both the strategies they use and how these unfold over time. Across 2 experiments, we examined the selection of exploratory procedures, the prioritisation of shape features, the temporal organisation of movement sequences, and how each of these aspects might be modulated by material properties. Together, our findings showed that although material properties influenced how participants explored shapes, they did not alter the shape relationships they ultimately perceived. Exploration strategies adapted flexibly to material contexts, while feature prioritisation, movement organisation, and perceptual judgements remained consistent, reflecting a balance between flexibility and stability in haptic shape perception.

Experiment 1 showed that exploration strategies varied with material properties, with tracing dominating EP patterns for both rigid and deformable objects. Deformable shapes elicited more diverse set of EPs, with tapping and scanning often used to supplement tracing. This pattern is consistent with previous findings showing contour following as the dominant EP for acquiring shape information [3, 33], but extends them by showing that participants flexibly incorporate additional EPs when object properties complicate exploration. The additional EPs likely were compensatory, helping participants stabilise their shape perception despite the challenges posed by the varying levels of compliance.

In line with this, interparticipant agreement was lower for deformable shapes, reflecting increased variability in judgements. Yet, similarity matrices across rigid and deformable conditions were strongly correlated, suggesting that while material variations introduced more individual variability in judgements, participants underlying shape representations were comparable. One possibility is that participants might have downweighed tactile cues linked to object properties unrelated to the task and relied more heavily on proprioceptive/kinematic feedback [34] and on stable geometrical cues to maintain consistent shape judgements. That is, they might have put more weight on the proprioceptive sensing of their movement path, used a coarse geometric abstraction of shape in that features are not exactly represented (e.g. only "sharp convexity"), or a combination of both. This idea fits reports on simplified shape representations in haptic perception [24-25]. Experiment 2 provided clearer evidence for a reliance on stable geometric features to guide perception. Using simplified stimuli without texture variations and a single deformability level, participants showed high agreement in their similarity judgements within conditions, and strong correlation across materials.

Exploration behaviours revealed a systematic preference for concave regions across all parameters, which is in line with the idea that concavities have highest perceptual saliency and may act as perceptual anchors that guide attention to shape-relevant information during exploration. At the same time the fact that participants revert to convexities suggests that these also have some perceptual relevance. In vision, concavities have been

shown to provide important structural information for defining part boundaries and facilitating shape recognition [18-19]. Their infrequent occurrence in close contours may enhance their perceptual value [35]. Further in vision, concavities are likely important for shape segmentation and object recognition. In active touch however the saliency of concavities could also serve other functions beyond segmentation and shape perception—reflecting properties that are potentially useful for biomechanic interaction and exploration: in particular, they involve abrupt changes in contour direction, may serve as natural reference points that help maintain orientation during exploration, and provide stable finger contact points. In line with the latter functions, our results on the left-right asymmetry of exploration suggests that the preference for concavity is shaped not only by geometry, but also by spatial accessibility. We found shape-specific effects and that concavities on the right side of the object were explored more extensively than those on the left, supporting a potential role of biomechanical constraints in feature prioritisation.

It is a related question how feature prioritization is controlled. We speculate this could be a process were first features are detected from sensory information, and then influence exploratory control in ways to enhance exploration intensity, probably by intentional small-range back and forth movements. This fits with the combination of higher velocities and longer distances travelled on concavities, and also with the reversal to convexities.

Participants also adjusted the applied force depending on the material properties; they applied more force to rigid shape and less to deformable shapes. This likely reflects an adaptive strategy in which, for rigid shapes, increased force may enhance tactile resolution, whereas reduced force helped avoid distortion in deformable shapes. Similar adaptive patterns were observed in the temporal sequence of exploration. While the overall structure of contour following remained stable across materials, with comparable numbers of reversal movements, participants also made more jumps between non-neighbouring regions when exploring deformable shapes and achieved greater contour coverage for rigid shapes. These results suggest that while the underlying exploration strategy was consistent, the execution of movement adapted flexibly to material constraints. These findings corroborate that the haptic system balances consistency with flexibility, maintaining stable exploration strategies for gathering shape information, while modulating the details of movements and force to accommodate material-specific task demands.

Together, the current experiments provided complementary insights into the organisation of haptic shape perception. Experiment 1 highlighted the flexibility of exploratory strategies, showing that material properties can diversify exploration strategies and reduce within condition agreement, yet still support consistent shape perception across rigid and deformable shapes. Experiment 2 demonstrated the stability of feature-based and temporally organised exploration, with participants prioritising concavities, maintained comparable contour-following patterns across materials, and achieved consistent judgements across material contexts. Across experiments, similarity matrices for rigid and deformable shapes were strongly correlated, and importantly, cross-experiment comparisons also showed overall high correlations (all $r^2 > .85$). This suggests that perceived shape relations were preserved not only within experiment, but also across different participant groups, stimuli, and task contexts.

IV. Conclusion

Overall, our results show that haptic shape perception is flexible in process but stable in outcome. Material properties influenced exploration through differences in exploratory procedures, force and movement patterns, but shape perception remains guided by consistent geometric cues, particularly concavities. This balance between adaptive exploration and stable feature prioritisation enables reliable shape information across diverse material contexts. Future work could explore the extent to which these stable exploration strategies generalise across a broader range of contexts. Understanding how haptic exploration remained flexible yet perceptually stable may inform design of haptic interfaces, robotic manipulators and assistive technologies that depend on efficient shape perception across materials.

References

[1] R. Klatzky, S. Lederman, and V. Metzger, “Identifying objects by touch: An ‘expert system’,” *Percept. Psychophys.*, vol. 37, no. 4, pp. 299–302, 1985.

[2] J. J. Gibson, “Observations on active touch,” *Psychol. Rev.*, vol. 69, no. 6, pp. 477–491, 1962.

[3] S. Lederman and R. Klatzky, “Hand movements: A window into haptic object recognition,” *Cogn. Psychol.*, vol. 19, no. 3, pp. 342–368, 1987.

[4] S. Lederman and R. Klatzky, “Extracting object properties through haptic exploration,” *Acta Psychol.*, vol. 84, no. 1, pp. 29–40, 1993.

[5] M. Cavdan, K. Doerschner, and K. Drewing, “Task and material properties interactively affect softness explorations along different dimensions,” *IEEE Trans. Haptics*, vol. 14, no. 3, pp. 603–614, 2021.

[6] D. Dövencioğlu, F. Üstün, K. Doerschner, and K. Drewing, “Hand explorations are determined by the characteristics of the perceptual space of real-world materials from silk to sand,” *Sci. Rep.*, vol. 12, no. 1, Art. no. 14785, 2022.

[7] I. E. Gordon and V. Morison, “The haptic perception of curvature,” *Percept. Psychophys.*, vol. 31, no. 5, pp. 446–450, 1982.

[8] J. Norman *et al.*, “Aging and curvature discrimination from static and dynamic touch,” *PLoS ONE*, vol. 8, no. 7, e68577, 2013.

[9] A. W. Goodwin, K. T. John, and A. H. Marceglia, “Tactile discrimination of curvature by humans using only cutaneous information from the fingerpads,” *Exp. Brain Res.*, vol. 86, no. 3, pp. 663–672, 1991.

[10] S. C. Pont, A. M. Kappers, and J. J. Koenderink, “The influence of stimulus tilt on haptic curvature matching and discrimination by dynamic touch,” *Perception*, vol. 27, no. 7, pp. 869–880, 1998.

[11] S. C. Pont, A. M. Kappers, and J. J. Koenderink, “Similar mechanisms underlie curvature comparison by static and dynamic touch,” *Percept. Psychophys.*, vol. 61, no. 5, pp. 874–894, 1999.

[12] H. Resnikoff, *The Illusion of Reality*. New York, USA: Springer, 2012.

[13] J. Norman, F. Phillips, and H. E. Ross, “Information concentration along the boundary contours of naturally shaped solid objects,” *Perception*, vol. 30, no. 10, pp. 1285–1294, 2001.

[14] M. Bertamini, “The importance of being convex: An advantage for convexity when judging position,” *Perception*, vol. 30, no. 11, pp. 1295–1310, 2001.

[15] M. Bertamini, M. Helmy, and J. Hulleman, “The role of convexity in perception of symmetry and in visual short-term memory,” *Q. J. Exp. Psychol.*, vol. 66, no. 4, pp. 767–785, 2013.

[16] J. Haushofer, C. I. Baker, M. S. Livingstone, and N. Kanwisher, “Privileged coding of convex shapes in human object-selective cortex,” *J. Neurophysiol.*, vol. 100, no. 2, pp. 753–762, 2008.

[17] G. Schmidtmann, B. J. Jennings, and F. A. A. Kingdom, "Shape recognition: Convexities, concavities and things in between," *Sci. Rep.*, vol. 5, Art. no. 17142, 2015.

[18] E. Barenholtz, E. H. Cohen, J. Feldman, and M. Singh, "Detection of change in shape: An advantage for concavities," *Cognition*, vol. 89, no. 1, pp. 1–9, 2003.

[19] J. Hulleman, W. T. Winkel, and F. Boselie, "Concavities as basic features in visual search: Evidence from search asymmetries," *Percept. Psychophys.*, vol. 62, no. 1, pp. 162–174, 2000.

[20] M. Bertamini, "Detection of convexity and concavity in context," *J. Exp. Psychol. Hum. Percept. Perform.*, vol. 34, no. 4, pp. 775–789, 2008.

[21] I. Biederman, "Recognition-by-components: A theory of human image understanding," *Psychol. Rev.*, vol. 94, no. 2, pp. 115–147, 1987.

[22] M. Bertamini and T. Farrant, "Detection of change in shape and its relation to part structure," *Acta Psychol.*, vol. 120, no. 1, pp. 35–54, 2005.

[23] J. M. Kennedy and R. Domander, "Shape and contour: The points of maximum change are least useful for recognition," *Perception*, vol. 14, no. 3, pp. 367–370, 1985.

[24] J. F. Soechting, W. Song, and M. Flanders, "Haptic feature extraction," *Cereb. Cortex*, vol. 16, no. 8, pp. 1168–1180, 2006.

[25] J. M. Ehrich, M. Flanders, and J. F. Soechting, "Factors influencing haptic perception of complex shapes," *IEEE Trans. Haptics*, vol. 1, no. 1, pp. 19–26, 2008.

[26] M. Wijntjes, K. Doerschner, G. Kucukoglu, and S. C. Pont, "Relative flattening between velvet and matte 3D shapes: Evidence for similar shape-from-shading computations," *J. Vis.*, vol. 12, no. 1, Art. no. 2, 2012.

[27] N. S. Chowdhury, P. J. Marlow, and J. Kim, "Translucency and the perception of shape," *J. Vis.*, vol. 17, no. 3, Art. no. 17, 2017.

[28] L. P. Y. Lin *et al.*, "Task-adapted single-finger explorations of complex objects," in *Proc. Int. Conf. Human Haptic Sens. Touch Enabled Comput. Appl. (EuroHaptics)*, 2024, pp. 133–146.

[29] L. P. Lin, K. Doerschner, and K. Drewing, "How shape and material properties affect touch patterns during complex shape perception," in *Proc. IEEE World Haptics Conf. (WHC)*, 2025, pp. 555–561.

[30] L. Kaim and K. Drewing, "Exploratory strategies in haptic softness discrimination are tuned to achieve high levels of task performance," *IEEE Trans. Haptics*, vol. 4, no. 4, pp. 242–252, 2011.

[31] P. Manjunatha, "CurvatureVisualize," GitHub repository, 2023. [Online]. Available: https://github.com/preethamam/CurvatureVisualize

[32] M. K. Driscoll *et al.*, "Cell shape dynamics: From waves to migration," *PLoS Comput. Biol.*, vol. 8, no. 3, e1002392, 2012.

[33] A. Withagen, A. M. Kappers, M. Vervloed, H. Knoors, and L. Verhoeven, "The use of exploratory procedures by blind and sighted adults and children," *Atten. Percept. Psychophys.*, vol. 75, pp. 1451–1464, 2013.

[34] V. Hayward, "Haptic shape cues, invariants, priors and interface design," in *Human Haptic Perception: Basics and Applications*. Basel, Switzerland: Birkhäuser, 2008, pp. 381–392.

[35] H. B. Barlow, "Possible principles underlying the transformation of sensory messages," in *Sensory Communication*. Cambridge, MA, USA: MIT Press, 1961, pp. 217–234.

[36] Y. Ujitoko, S. Sakurai, and K. Hirota, "Influence of sparse contact point and finger penetration in object on shape recognition," *IEEE Trans. Haptics*, vol. 13, no. 2, pp. 425–435, 2020.

Lisa Lin received the Ph.D. degree in Psychology from Lancaster University, United Kingdom, in 2022. She is currently a Postdoctoral Researcher in the Department of Psychology at Justus-Liebig-University, Giessen, Germany. Her research interests include visual and haptic material perception, as well as the role of the body and its action capabilities in visual perception.

Alap Kshirsagar received the Ph.D. degree in Mechanical Engineering from Cornell University, USA, in 2022. He is currently a Postdoctoral Researcher in the Computer Science Department at TU Darmstadt, Germany. His research interests include human-robot interaction, robotic manipulation, and tactile perception.

Boris Belousov received the Ph.D. degree in Computer Science from TU Darmstadt, Germany, in 2022. He was a Senior Researcher and Deputy Head at the German Research Center for Artificial Intelligence department on Systems AI for Robot Learning (DFKI-SAIROL) till 2025. His research interests include reinforcement learning, model predictive control, tactile sensing, robotic manipulation.

Tim Schneider received the M.Sc. degree in Computer Science from TU Darmstadt, Germany, in 2021. He is currently a Ph.D. student in the Computer Science Department at Technical University of Darmstadt, Germany. His research interests include active perception, tactile sensing, and robotic manipulation.

Jan Peters, (Fellow, IEEE) received the Ph.D. degree in Computer Science from the University of Southern California, USA, in 2007. He is a full Professor (W3) of Intelligent Autonomous Systems with the Computer Science Department, TU Darmstadt, Germany, Department Head of the research department on Systems AI for Robot Learning (DFKI-SAIROL), German Research Center for Artificial Intelligence, Germany, and a founding Research Faculty Member of The Hessian Center for Artificial Intelligence, Germany. His research interests include robot learning, robotics, machine learning, cognitive science, biomimetic systems.

Katja Doerschner received her Ph.D. in Experimental Psychology from New York University, USA. She is currently a Professor at the Department of Psychology and PI of the perception and active exploration (PACE) group at Justus-Liebig-University, Germany. Her research focuses on understanding how active explorations with eyes and hands shape the perception of object properties.

Knut Drewing received the Ph.D. in psychology from LMU Munich in 2001, and the Postdoctoral Lecture Qualification in psychology from JLU Giessen, Germany, in 2010. He was with the MPIs for psychological research, Munich and for Biological Cybernetics, Tuebingen. He is an Associate Editor-in-Chief for IEEE Transactions on haptics, a Professor with the Department of Psychology, and Leader of HapLab, JLU Giessen. His research interests include haptic perception, multisensory integration, time perception.